Malaysian Journal of Fundamental and Applied Sciences Vol.9, No.2 (2013) 67-73

ISSN 1823-626X

**Malaysian Journal of Fundamental and Applied Sciences**

**available online at http://mjfas.ibnusina.utm.my**

# Photodecolorization of methylene blue over $EGZrO_2/EGZnO/EGFe_2O_3/HY$ photocatalyst: Effect of radical scavenger

N. Sapawe[1], A.A. Jalil[1]* and S. Triwahyono[2]

[1]Institute of Hydrogen Economy, Faculty of Chemical Engineering, Universiti Teknologi Malaysia, 81310 UTM Johor Bahru, Johor, MALAYSIA
[2]Ibnu Sina Institute for Fundamental Science Studies, Dept. of Chemistry, Fac. of Science, Universiti Teknologi Malaysia, 81310 UTM Johor Bahru, Johor, MALAYSIA

Received 1 November 2012, Revised 2 February 2013, Accepted 26 February 2013, Available online 3 March 2013

## ABSTRACT

The photocatalytic activity of methylene blue (MB) was investigated in aqueous solutions under solar radiation using electrogenerated metals supported on HY zeolite ($EGZrO_2/EGZnO/EGFe_2O_3/HY$) catalyst. The prepared catalysts were examined using X-ray diffraction (XRD), transmission electron microscopy (TEM), and Brunnauer-Emmett-Teller surface area analysis (BET). An amount of 0.375 g $L^{-1}$ $EGZrO_2/EGZnO/EGFe_2O_3/HY$ was found to be the optimum dosage for 10 mg $L^{-1}$ MB, which gave almost complete photodecolorization of MB (99.5%) after 1 h of contact time at pH 9. Next, the effect of inorganic salts such as NaCl, $Na_2CO_3$, $Na_2SO_4$, and KI was also studied. It was found that the presence of the $Cl^-$ and $CO_3^{-2}$ ions obstructed the photodecolorization, but the presence of $SO_4^{2-}$ accelerated the reaction. The presence of $I^-$ ions did not affect much on the decolorization rate. Furthermore, the addition of $H_2O_2$ significantly enhanced the photodecolorization for the 50 mg $L^{-1}$ of MB solution under similar optimum conditions. It was also found that the radical scavenging agents such as dimethyl sulfoxide (DMSO) and methanol (MeOH) suppressed the decolorization, with DMSO being the most effective. The simple preparation of the photocatalyst and low amount of metal loading required exhibits the great potential of the system that could be applied in textile or other industries wastewater treatment.

| $EGZrO_2/EGZnO/EGFe_2O_3/HY$ | photocatalyst | methylene blue | decolorization | solar radiation |

http://dx.doi.org/10.11113/mjfas.v9n2.85

## 1. INTRODUCTION

Environmental problem involving water pollution has become an important issue nowadays. Organic dyes are the major pollutants in wastewater which are produced from the dyeing processes. About 15% of the total world production of dyes is released in the textile effluents, with nearly 97% of local dye effluents are produced by the food, chemical, and textile industries [1–4]. Most of the unused dye results in undesirable effluents are discharged into the environment with or without further treatment. These effluents run into natural water bodies can cause severe problems if not treated properly because the dyes are toxic, mutagenic and carcinogenic to human life, as well as prohibit the photosynthesis of aquatic life when present even in small quantities like 1 ppm [3–7]. To overcome this problem, several methods for the removal of dyes have been reported including chemical and biological oxidation, adsorption, coagulation and flocculation, electrochemical oxidation, ion exchange, and membrane separation [8–14]. These methods have their own limitations including being time–consuming, expensive, and commercially unattractive as well as resulting in the generation of secondary wastes.

The use of metal oxide semiconductor such as $TiO_2$, ZnO, $WO_3$, $Fe_2O_3$, CuO, $ZrO_2$, CdS, $In_2O_3$, and $SnO_2$ as a photocatalyst under advanced oxidation processes (AOPs) have become crucial because the AOPs can convert a wide range of harmful dyes into non–toxic products, $CO_2$ and water at ambient temperature [3–7]. Further, the use of mixed metal oxides such as $TiO_2$–$ZrO_2$, Ag–ZnO, $Fe_2O_3$–$TiO_2$, $TiO_2$–ZnS, Sn–ZnO, and Ag–$TiO_2$ have been recognized to exhibit better performance, and enhances the photocatalytic activity [15–20]. To date, few studies have been reported based on the use of more than two metal oxides as the photocatalyst. The mesoporous materials such as zeolite as a support for the metal oxides have recently become the focus of intensive research because the catalyst support influences the catalytic performance through structural features [3–7,21]. In addition, the interaction between the materials leads to the enhancement of the contact between the surface and irradiation, as well as reduction in the amount of metal oxides required [3–7]. Zeolitic supports are important because of their high surface area, thermal stability, eco–friendly nature, specific photophysical properties, and their potential ability to control charge and electron transfer processes [3].

A review of current studies has revealed that some of the essential metal oxide–supported zeolites include $TiO_2$–HZSM–5, Co–ZSM–5, CuO–X zeolite, and Fe–exchange zeolite [20,22–24]. The most frequent metal oxide use is $TiO_2$ and ZnO, but alternative photocatalyst are still under development and more research is required. The ZnO nanoparticles have evoked a great deal of interest in the area of photocatalytic studies for enhancing the performance

---

*Corresponding author. Email: aishah@cheme.utm.my
(A.A. Jalil) Tel: (+60)-7-5535581, Fax: (+60)-7-5536165

such increased in the surface area and changes in surface properties as well as quantum effect of the photocatalyst materials [6,7]. In the other hand, the utilization of $Fe_2O_3$ as tremendous photocatalyst also have been widely studied due to their unique properties such as size in nano–range, high surface area to volume ratios, superparamagnetism, low toxicity, chemically inertness, and biocompatibility [25–27]. Furthermore, $ZrO_2$ shows good specific optical and electrical properties, thermal stability, and strong mechanical strength as well as the presence of acid–base and redox capabilities [3,4]. However, the development of more than two metal oxides supported HY catalyst is still scarce.

We have reported on the preparation method for an α–$Fe_2O_3$, EG$ZrO_2$ and EGZnO supported HY catalyst by a simple and rapid electrochemical process, which possesses high photoactivity in the decolorization of methyl orange and methylene blue, respectively [3–7]. The nanosized metal oxides as well as the synergistic interaction between the metal and the support were found to play important roles in the enhancement of the reaction [21]. Further study on the property of that zinc metal oxide showed that it was nanoparticle in size, which showed promising photoactivity in the removal of methyl orange and methylene blue from aqueous solutions [6,7]. By the corresponding method, we have succeeded to generate a very fine particles metal with higher reactivity. The introduction of several metal oxides presumably could be improved and endowed extra properties to the photocatalyst by altering and restructuring the materials.

Herein, we attempted to prepare $ZrO_2$, ZnO, and $Fe_2O_3$ supported on HY zeolite by the corresponding method which is fast, simple and efficient than other methods with the aim to reduce amount of metal oxide used and tested its photoactivity on the decolorization of methylene blue (MB), towards a green environment. The prepared catalysts were characterized by X-ray diffraction (XRD), transmission electron microscopy (TEM), and Brunnauer-Emmett-Teller of surface area analysis (BET). The effect of radical scavengers using several of inorganic salts ($Na_2SO_4$, $Na_2CO_3$, NaCl, and KI), hydrogen peroxide ($H_2O_2$), dimethyl sulfoxide (DMSO), and methanol (MeOH) were also investigated in details towards the MB decolorization simultaneously with the mechanism of reaction.

## 2. EXPERIMENTAL

### 2.1 Materials

The HY zeolite had a Si/Al ratio of 80 and was purchased from the Zeolyst International. *N,N*–dimethylformamide (DMF) was purchased from Merck and naphthalene was obtained from Fluka. Sodium hydroxide, hydrochloric acid, methanol, hydrogen peroxide, methylene blue, sodium carbonate, sodium sulphate, sodium chloride, and potassium iodide were obtained from QReC™. The dimethyl sulfoxide (DMSO) was purchased from Sigma-Aldrich, Inc. The platinum (Pt), zirconia (Zr), zinc (Zn), and iron (Fe) plate cells were obtained from Nilaco Metal, Japan. All reagents were of analytical grade and were used as received. Deionized water was used for the preparation of the pH solution and adjustments to the pH were performed using a 0.1M HCl and NaOH solution.

### 2.2 Catalyst preparation

The 1 wt% EG$ZrO_2$/1 wt% EGZnO/1 wt% EG$Fe_2O_3$/HY catalyst was prepared using a 10 mL of DMF solution which containing of 0.1 M tetraethylammonium perchlorate (TEAP), electrolyzed in the presence of a naphthalene mediator (6 mmol) and HY zeolite (1.5 g) in a normal one–compartment cell fitted with a Pt plate cathode (2 × 2 $cm^2$) and Zr, Zn, and Fe anode plates (2 × 2 $cm^2$ each) at a constant current density of 120 mA/$cm^2$ under a nitrogen atmosphere at 273 K [28–30]. The anodes were used alternately as Zr, Zn and Fe, depending on the amount required. After electrolysis, the mixture was impregnated, oven dried overnight at 378 K, and calcined at 823 K for 3 h to yield a brownish powder EG$ZrO_2$/EGZnO/EG$Fe_2O_3$/HY catalyst, which ready for characterization and photocatalytic testing. The required weight percent of the EG$ZrO_2$, EGZnO, and EG$Fe_2O_3$ supported on HY, and the time required for complete electrolysis was calculated based on Faraday's law of electrolysis,

$$t = \left(\frac{F}{I}\right)(z \times n) \tag{1}$$

where $t$ = total time for the constant current applied (s); $F$ = 96486 C $mol^{-1}$, which is the Faraday constant; $I$ = the electric current applied; $z$ = the valency number of ions of substances (electrons transferred per ion); and $n$ = the amount of substance (no of moles, liberated n = m/M).

### 2.3 Characterization

The crystalline structures of the catalysts were studied by XRD recorded on a D8 ADVANCE Bruker X–ray diffractometer using Cu $K_\alpha$ radiation at a 2θ angle ranging from 3° to 90°. The particle sizes of the catalysts were calculated using the Debye–Scherrer equation,

$$D = \frac{k\lambda}{\beta \cos\theta} \tag{2}$$

where $k$ = 0.94 is a coefficient, λ = 1.5406 Å is the X–ray wavelength, $\beta$ is the full width half maximum (FWHM) of the sample and θ is the diffracting angle. The phases were identified with the aid of the Joint Committee on Powder Diffraction Standards (JCPDS) files.

The morphological properties of the prepared EG$ZrO_2$/EGZnO/EG$Fe_2O_3$/HY catalyst, and the distribution of $EGZrO_2/EGZnO/EGFe_2O_3$ deposited on the HY surface were examined by TEM (JEOL JEM–2100F). The textural properties (i.e., specific surface area, pore volume, and pore diameter) were determined from nitrogen adsorption–desorption isotherms at liquid nitrogen temperature using a Micromeritics ASAP 2010 instrument. The surface area was calculated with the BET method, and pore distributions were determined by the Barrett–Joyner–Halender (BJH) method. Prior to measurement, all the samples were degassed at 383 K to 0.1 Pa.

## 2.4 Reaction testing

The photocatalytic activity of the prepared $EGZrO_2/EGZnO/EGFe_2O_3/HY$ catalyst was tested for the decolorization of MB. A 0.075 g of the catalyst was dispersed in 200 mL of 10 mg $L^{-1}$ MB aqueous solution. The adsorption–desorption equilibrium was achieved under dark conditions after 1 h, and the mixture was then exposed for 1 h with constant stirring under sunlight (January to March 2012, between 12 NN until 3 PM). The average intensity of sunlight during this period is 1.315 x $10^5$ Lux unit. Irradiation was carried out in the open air condition. However, during the illumination time, no volatility of the solvent was observed.

At specific time intervals, 2.5 mL of the sample solution was withdrawn and centrifuged prior measurements for the remaining MB concentration by a UV–vis spectrophotometer (Agilent Technologies Cary 60 UV–vis) using the characteristic adsorption band at 664 nm. The decolorization percentage was calculated as follows,

$$Decolorization\ (\%) = \frac{(C_0 - C_t)}{C_0} \times 100 \qquad (3)$$

where $C_o$ represents the initial concentration and $C_t$ denotes a variable concentration.

## 3. RESULTS & DISCUSSION

The XRD pattern of $EGZrO_2/EGZnO/EGFe_2O_3/HY$ catalyst was compared with bare HY, and the results are shown in Fig. 1. The peak intensity of HY was decreased as the $EGZrO_2$, EGZnO, and $EGFe_2O_3$ metal oxide were loaded because the presence of foreign substances affected the morphology of the supported HY fingerprint. The enlargement of a selected area of the XRD pattern from 22° to 72° shows several peaks detected corresponding to $ZrO_2$, ZnO, and $Fe_2O_3$, verifying the presence of $EGZrO_2$, EGZnO, and $EGFe_2O_3$ metals on the HY support.

On the basis of the major peaks of $EGZrO_2$ (101), EGZnO (101), and $EGFe_2O_3$ (104), the average crystallite size of the catalysts was estimated by the Debye–Scherrer equation, which were 11.7 nm, 30.2 nm, and 26.5 nm, respectively. However, upon to the formation of the $EGZrO_2/EGZnO/EGFe_2O_3$ catalyst, this crystallite size was increased to 13.6 nm, 32.8 nm, and 28.5 nm, respectively. This may be due to agglomeration and the interaction between the zirconia, zinc, and iron species [3–7].

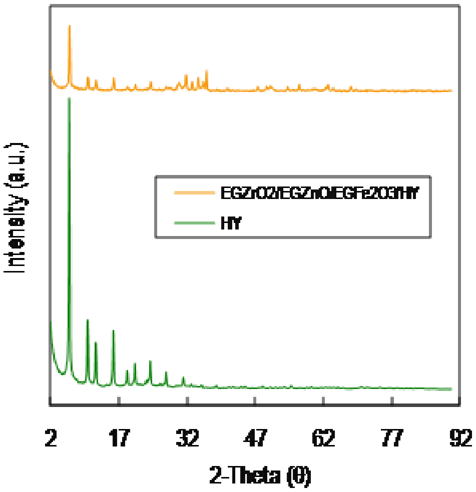

**Fig. 1.** XRD patterns of photocatalysts for full range 2–92°.

The surface area analysis data obtained from the BET method, and the pore volume and pore diameter determined by the Barret–Joyner–Halenda (BJH) desorption isotherms method were tabulated in Table 1. The addition of $EGZrO_2/EGZnO/EGFe_2O_3$ onto HY increased the surface area, pore diameter, and pore volume, which might due to the existence of electrogenerated metal oxide nanoparticles. It was hypothesized that improvement in the surface contact of the photocatalyst enhanced the light irradiation, thereby increasing the photodecolorization of MB. A similar observation was also reported for the photoreduction of methyl orange by $TiO_2$ supported on a zeolite matrix [31].

**Table 1.** The textural properties of the photocatalysts.

| Photocatalyts | Surface area ($m^2g^{-1}$) | Average pore diameter[a] (nm) | Pore volume ($cm^3g^{-1}$) |
|---|---|---|---|
| HY | 557 | 2.70 | 0.376 |
| $EGZrO_2/EGZnO/$<br>$EGFe_2O_3/HY$ | 636 | 2.90 | 0.462 |

[a] Adsorption average pore diameter (4V/V by BET)

The morphological properties of the prepared $EGZrO_2/EGZnO/EGFe_2O_3/HY$ catalyst were examined by transmission electron microscopy (TEM), and the images are presented in Fig. 2. The inset figures correspond to the fast Fourier transform patterns (FFT), and indicated that the material is crystalline phase. Magnification of the selected area in the FFT patterns showed the atomic arrangement in the crystal, and allowed the estimation of the interplanar distances. The value of the interplanar distance (*d*–spacing) of the lattice fringes estimated from this image was consistent with the value of the lattice spacing of $EGZrO_2$, EGZnO, and $EGFe_2O_3$ which is available in the XRD database. In addition, the existence of black spot confirms that the $EGZrO_2$, EGZnO, and $EGFe_2O_3$ nanoparticles were well dispersed on the HY support.

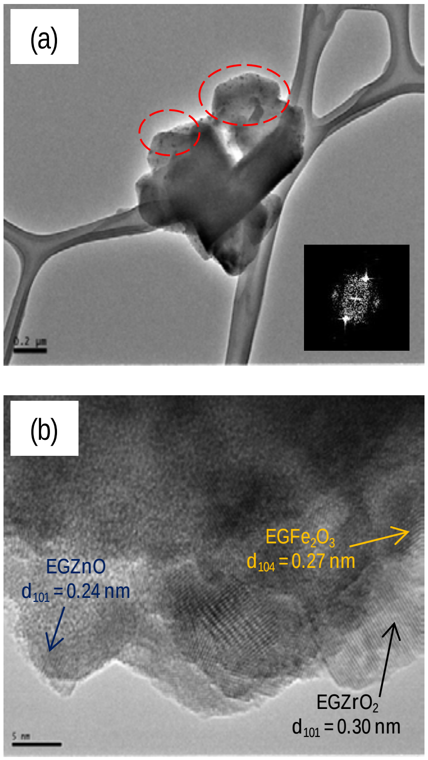

**Fig. 2.** TEM micrographs of 1 wt% $EGZrO_2$/1 wt% EGZnO/1 wt% $EGFe_2O_3$/HY photocatalyst, and the inset figure is its corresponding FFT.

The photocatalytic activity of the prepared $EGZrO_2$/EGZnO/$EGFe_2O_3$/HY catalyst was tested, and compared with bare HY and $EGZrO_2$/EGZnO/$EGFe_2O_3$ catalyst on the decolorization of MB; the results are shown in Fig. 3. Each experiment was performed in the dark to achieve adsorption–desorption equilibrium before exposure to sunlight for 1 h with constant stirring. The results show that almost complete decolorization of MB was achieved within a short period (1 h) of contact time when using $EGZrO_2$/EGZnO/$EGFe_2O_3$/HY, compared with the two others examined catalysts, 10.1% and 35.6%, respectively, indicating the high photoactivity of the prepared photocatalyst under sunlight irradiation. The photolysis study of MB was also conducted, and it shows that less significant of MB decolorization was occurred.

The effect of sulphate ion (electron scavenger) on the photocatalytic decolorization of the MB was then investigated by varying its amount from 0.5 to 2.0 g $L^{-1}$, and was presented in Fig. 4. The percentage decolorization of the MB increases with increasing amount of sulphate ion which may be attributed to the beneficial oxidizing agent in the photocatalytic detoxification to form sulphate radical anion ($SO_4^{\cdot-}$) from the oxidant by reactions Eqs. (4) and (5) with the electrons generated in the conduction band ($e^-_{cb}$) of $EGZrO_2$/EGZnO/$EGFe_2O_3$/HY semiconductor.

$$S_2O_8^{2-} + e^-_{aq} \rightarrow SO_4^{-\bullet} + SO_4^{2-} \qquad (4)$$

$$S_2O_8^{2-} + e^-_{cb} \rightarrow SO_4^{-\bullet} + SO_4^{2-} \qquad (5)$$

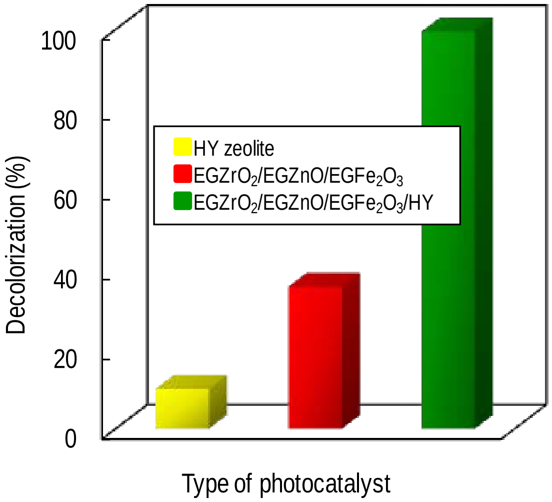

**Fig. 3.** Photocatalysts performance on decolorization of MB. ($C_{MB}$ = 10 mg $L^{-1}$, pH 9, W = 0.375 g $L^{-1}$, t = 1 h, under sunlight)

The sulphate radical anion ($SO_4^{\cdot-}$) is a strong oxidant ($E^0$ = 2.6 eV), and engages in the following three possible modes of reactions with organic compounds: (i) by abstracting a hydrogen atom from saturated carbon, (ii) by adding hydrogen to unsaturated or aromatic carbon, and (iii) by removing one electron from the carboxylate anion and from certain neutral molecules [32]. In addition, it can trap the photogenerated electrons and/or generate hydroxyl radical [32–34].

$$SO_4^{-\bullet} + e^-_{cb} \rightarrow SO_4^{2-} \qquad (6)$$

$$SO_4^{-\bullet} + H_2O \rightarrow {}^{\bullet}HO + SO_4^{2-} + H^+ \qquad (7)$$

The $SO_4^{\cdot-}$ and $^{\cdot}OH$ radicals are powerful oxidants that can degrade the dye molecules at faster rate. The $SO_4^{\cdot-}$ has unique nature of attacking the dye molecule at various positions, and therefore the fragmentation of the dye molecules is rapid.

$$SO_4^{-\bullet} + dye \rightarrow SO_4^{2-} + dye^{+\bullet}\ (\text{int}\,ermediates) \qquad (8)$$

$$SO_4^{-\bullet} + dye^{+\bullet}\ (\text{int}\,ermediates) \rightarrow SO_4^{2-} + CO_2 + HNO_3 + other\ organics \qquad (9)$$

Sodium carbonate is the common auxiliary chemical that employed in textile processing operations; mainly used in the dyeing bath to adjust the pH of the bath as it plays an important role in fixing the dye on the fabrics and in the fastness of colour. Therefore, wastewater from the dyeing operation contains considerable amount of carbonate ion. The effect of carbonate ion was investigated, and results show that the percentage of decolorization was gradually decreased with increasing carbonate ion concentration (Fig. 4). The decrease in the decolorization of MB might due to the hydroxyl scavenging property of carbonate ions which can be accounted from the following reactions [35],

$$ {}^\bullet OH + CO_3^{2-} \rightarrow OH^- + CO_3^{-\bullet} \qquad (10) $$

$$ {}^\bullet OH + HCO_3^- \rightarrow H_2O + CO_3^{-\bullet} \qquad (11) $$

Similar trend was also observed in the photocatalytic degradation of reactive dyes [36]. Behar and his co–workers reported the possibility of generating carbonate radical anions ($CO_3^{-\cdot}$) assist by the hydroxyl radicals [37]. The free hydroxyl radical (primary source or oxidant) decreased gradually with increased in carbonate ions, and ultimately decreases in the percentage of decolorization.

Another common interfering inorganic ion is chloride ion (sodium chloride), which usually comes out in the effluents along with sectional wastes of textile mills. Photocatalytic studies have been carried out using sodium chloride in the range of 0.5 to 2.0 g $L^{-1}$ (Fig. 4). It was observed the percentage decolorization of MB decreased with increased in the amount of chloride ion. The results are in good agreement with those published by Abdullah and his co–workers who reported a strong inhibiting effect of chloride and phosphate ions [38]. It is due to the hole scavenging properties of chloride ion as shown in the following Eqs. (12) – (16). This is a typical example for competitive inhibition. The reaction of dye molecules with the holes will have to compete with this reaction [39].

$$ ZrO_2 \rightarrow ZrO_2\ (h^+_{vb} + e^-_{cb}) \qquad (12) $$

$$ ZnO \rightarrow ZnO\ (h^+_{vb} + e^-_{cb}) \qquad (13) $$

$$ Fe_2O_3 \rightarrow Fe_2O_3\ (h^+_{vb} + e^-_{cb}) \qquad (14) $$

$$ Cl^- + h^+_{vb} \rightarrow Cl^\bullet \qquad (15) $$

$$ Cl^\bullet + Cl^- \rightarrow Cl_2^{-\bullet} \qquad (16) $$

As chlorine radicals are forming slowly, they are instantaneously converted into chloride radical anion. Instead, surface sites normally available at the $EGZrO_2$/ EGZnO/$EGFe_2O_3$/HY/dye solution, interface for adsorption and electron transfer from the dye can be blocked by anions such as chloride and phosphate which are not readily oxidizable, but yet very effective inhibitors for the detoxification process. The catalyst was washed with pure water to restore its photocatalytic activity, when chloride ions are present in the wastewater.

Iodide ion is a scavenger that reacts with positive holes and surficial hydroxyl radicals (Eqs. (17) and (20)), reducing the number of oxidizing species available on the catalyst surface for reaction with dyes [40].

$$ I^- + h^+_{vb} \rightarrow I^\bullet \qquad (17) $$

$$ I^\bullet + I^- \rightarrow I_2^{-\bullet} \qquad (18) $$

$$ I_2^{\bullet -} + e^-_{cb} \rightarrow I_2 \qquad (19) $$

$$ I^- + {}^\bullet OH_s \rightarrow I^\bullet + OH_s^- \qquad (20) $$

$$ {}^\bullet OH_s + I_2 \rightarrow HOI + I^\bullet \qquad (21) $$

Fig. 4 also demonstrated the change of photocatalytic decolorization of MB with increasing KI concentration to 1.0 g $L^{-1}$, since iodide ion scavenged the positive holes and surficial hydroxyl radicals on catalysts surface to reduce the number of reactive species available for decolorization of the MB. Further increase in KI concentration seems did not affect much on the decolorization of MB. In addition, iodide ion compete the active sites on the $EGZrO_2$/EGZnO/ $EGFe_2O_3$/HY surface with MB, resulting less efficiency on the decreasing of photodecolorization.

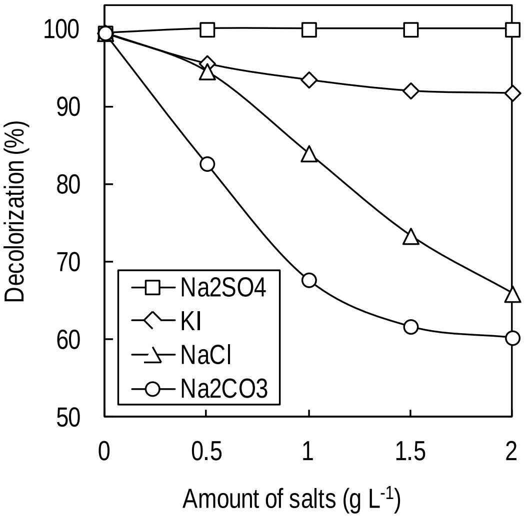

**Fig. 4** Effect of inorganic salts on decolorization of MB. ($C_{MB}$ = 10 mg $L^{-1}$, pH 9, W = 0.375 g $L^{-1}$, t = 1 h, under sunlight)

Significantly, the photoassisted degradation of organic substrates could be improved in the presence of hydrogen peroxide ($H_2O_2$). The presence of $H_2O_2$ in the reaction mixture will play an important role in the photocatalytic processes since that the reactive hydroxyl radicals are easily generated by the breakdown of $H_2O_2$ [41]. To study this effect, $H_2O_2$ was added in the 50 mg $L^{-1}$ MB solutions in the concentration range of 1 to 20% v/v, and was shown in Fig. 5a. Almost complete decolorization has been achieved within 1 h irradiation in the presence of 5% v/v $H_2O_2$. It has been widely reported that the addition of small amount of $H_2O_2$ greatly enhances the oxidation of organic pollutants mediated by $TiO_2$ catalyst [41].

The enhanced photodegradation efficiency in the presence of $H_2O_2$ may be either directly via conduction band electrons or indirectly via superoxide radical anion which produces hydroxyl radicals [42]. The following Eqs. (22) – (25) implies the addition of $H_2O_2$ during the reaction increased the rate of decolorization.

$$H_2O_2 + e^- \rightarrow {}^\bullet OH + HO^- \tag{22}$$

$$H_2O_2 + O_2^{-\bullet} \rightarrow {}^\bullet OH + HO^- + O_2 \tag{23}$$

$$H_2O_2 \rightarrow 2{}^\bullet OH \tag{24}$$

$$H_2O_2 \rightarrow O_2^{2-} + 2H^+ \tag{25}$$

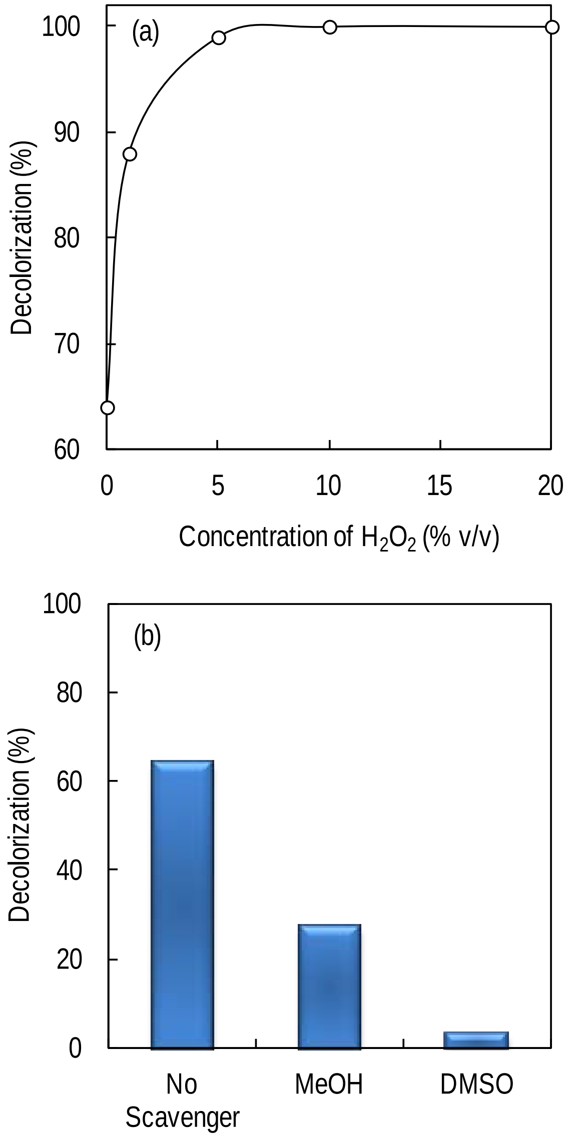

**Fig. 5** Effect of (a) hydrogen peroxide, and (b) other scavenging agents (10% v/v) on decolorization of MB. ($C_{MB}$ = 50 mg $L^{-1}$, pH 9, W = 0.375 g $L^{-1}$, t = 1 h, under sunlight)

In addition, the effect of scavenging agents such as dimethyl sulfoxide (DMSO) and methanol (MeOH) towards the decolorization of MB was also conducted under similar conditions using 10% v/v of concentration. As shown in Fig. 5b, the addition of the radical scavenging agents for both DMSO and MeOH significantly suppressed the degradation of MB, possibly by quenching the $^\cdot$OH radicals. Among the scavengers, DMSO was the most effective. The decolorization of MB after 1 h irradiation was 64.0% in absence of $^\cdot$OH scavenging agent (control), while addition of MeOH and DMSO suppressed the decolorization of MB to be 27.3% and 3.1%, respectively. A similar phenomenon was also reported by Shimizu and his co–workers [43]. Thus, the results from these studies demonstrated that $^\cdot$OH radicals may play an important role in the decolorization of MB.

## 4. CONCLUSIONS

In this study, 1 wt% $EGZrO_2$/1 wt% EGZnO/1 wt% $EGFe_2O_3$/HY photocatalyst was prepared by a simple electrochemical method. The physicochemical properties of the prepared photocatalyst were studied by XRD, TEM, and BET surface area. Nearly complete photodecolorization of MB (99.5%) was obtained using an amount of 0.375 g $L^{-1}$ photocatalyst for 10 mg $L^{-1}$ MB after 1 h of contact time at pH 9. It was found that the presence of the $Cl^-$ and $CO_3^{-2}$ ions are hindering the photodecolorization activity, but the presence of $SO_4^{2-}$ accelerated the reaction. However, the presence of $I^-$ ions did not affect much on the decolorization rate. The following mechanisms of photoreaction were discussed in details. Significantly, the addition of $H_2O_2$ gave a major role in enhancing photodecolorization of 50 mg $L^{-1}$ of MB solutions under similar reaction conditions. The radical scavenging agents such as DMSO and MeOH was suppressed the photodecolorization, with DMSO being the most effective. Facile preparation method with low amount of metal loading could exhibits a great potential to this system to be applied in textile or other industries wastewater treatment. The photocatalytic decolorization of dyes employing sunlight irradiation may emerge as a viable method because of its eco–friendliness and cost effective.

## ACKNOWLEDGEMENT

The authors are grateful for the financial support by the Research University Grant from Universiti Teknologi Malaysia (Grant No. 01H59), the awards of UTM Zamalah Scholarship (Norzahir Sapawe) and the Hitachi Scholarship Foundation for their support.

## REFERENCES

[1] S. Ameen, M.S. Akhtar, Y.S Kim, H.S. Shin, Appl. Catal. B: Environ. 103 (2011) 136–142.

[2] A. Houas, H. Lachheb, M. Ksibi, E. Elaloui, C. Guillard, J.M. Herrmann, Appl. Catal. B: Environ. 31 (2001) 145–157.

[3] N. Sapawe, A.A. Jalil, S. Triwahyono, S.H. Adam, N.F. Jaafar, M.A.H. Satar, Appl. Catal. B: Environ. 125 (2012) 311–323.

[4] N. Sapawe, A.A. Jalil, S. Triwahyono, J. Fundamental Sci. 7 (2011) 137–139.

[5] N.F. Jaafar, A.A. Jalil, S. Triwahyono, M.N.M. Muhid, N. Sapawe, M.A.H. Satar, H. Asaari, Chem. Eng. J. 191 (2012) 112–122.

[6] N. Sapawe, N.F. Jaafar, N.H.H. Hairom, M.A.H. Satar, M.N. Ariffin, S. Triwahyono, A.A. Jalil, J. Fundamental Sci. 7 (2011) 19–23.

[7] N. Sapawe, A.A. Jalil, S. Triwahyono, R.N.R.A. Sah, N.W.C. Jusoh, N.H.H. Hairom, J. Efendi, Electrochemical strategy for grown ZnO nanoparticles deposited onto HY zeolite with enhanced photodecolorization of methylene blue: Effect of the formation of Si–O–Zn bonds, *Applied Catalysis A, General* (2013), http://dx.doi.org/10.1016/j.apcata.2013.02.025

[8] C.S.D. Rodrigues, L.M. Madeira, R.A.R. Boaventura, J. Hazard. Mater. 172 (2009) 1551–1559.

[9] A.A. Jalil, S. Triwahyono, M.R. Yaakob, Z.Z.A. Azmi, N. Sapawe, N.H.N. Kamarudin, H.D. Setiabudi, N.F. Jaafar, S.M. Sidik, S.H. Adam, B.H. Hameed, Bioresource Technol. 120 (2012) 218–224.

[10] A.A. Jalil, S. Triwahyono, S.H. Adam, N.D. Rahim, M.A.A. Aziz, N.H.H. Hairom, N.A.M. Razali, M.A.Z. Abidin, M.K.A. Mohamadiah, J. Hazard. Mater. 181 (2010) 755–762.

[11] F. Harrelkas, A. Azizi, A. Yaacoubi, A. Benhammou, M.N. Pons, Desalination 235 (2009) 330–339.

[12] M. Panizza, G. Cerisola, Appl. Catal. B: Environ. 75 (2007) 95–101.

[13] J.S. Wu, L.H. Liu, K.H. Chu, S.Y. Suen, J. Membr. Sci. 309 (2008) 239–245.

[14] R.A. Damodar, S.J. You, S.H. Ou, Sep. Purif. Technol. 78 (2010) 64–71.

[15] W. Zhou, K. Liu, H. Fu, K. Pan, L. Zhang, L. Wang, C.C. Sun, Nanotechnol. 19 (2008) 1–7.

[16] M.J. Height, S.E. Pratsinis, O. Mekasuwandumrong, P. Praserthdam, Appl. Catal. B: Environ. 63 (2006) 305–312.

[17] X. Yang, C. Cao, L. Erickson, K. Hohn, R. Maghirang, L. Klabunde, Appl. Catal. B: Environ. 91 (2009) 657–662.

[18] A. Franco, M.C. Neves, M.M.L. Mobteiro, J. Hazard. Mater. 161 (2009) 545–550.

[19] J.H. Sun, S.Y. Dong, J.L. Feng, X.J. Yin, X.C. Zhao, J. Mol. Catal. A: Chem. 335 (2011) 145–150.

[20] W. Zhao, L. Feng, R. Yang, J. Zheng, X. Li, Appl. Catal. B: Environ. 103 (2011) 181–189.

[21] S. Triwahyono, A.A. Jalil, M. Musthofa, Appl. Catal. A: Gen. 372 (2010) 90–93.

[22] Z.M. El–Bahy, M.M. Mohamed, F.I. Zidan, M.S. Thabet, J. Hazard. Mater. 153 (2008) 364–371.

[23] A. Nezamzadeh–Ejhieh, S. Hushmandrad, Appl. Catal. A: Gen. 388 (2010) 149–159.

[24] R. Prihodko, I. Stolyarova, G. Gunduz, O. Taran, S. Yashnik, V. Parmon, V. Guncharuk, Appl. Catal. B: Environ. 104 (2011) 201–210.

[25] A.K. Gupta, M. Gupta, Biomaterials 26 (2005) 3995–4021.

[26] S.H. Huang, M.H. Liao, D.H. Chen, Biotechnol. Prog. 19 (2003) 1095–1100.

[27] M.C. Roco, Curr. Opin. Biotechnol. 14 (2003) 337–346.

[28] A.A. Jalil, N. Kurono, M. Tokuda, Synlett. 12 (2001) 1944–1946.

[29] A.A. Jalil, N. Kurono, M. Tokuda, Tetrahedron 58 (2002) 7477–7484.

[30] A.A. Jalil, N. Kurono, M. Tokuda, Synthesis 18 (2002) 2681–2686.

[31] R. Chatti, S.S. Rayalu, N. Dubey, N. Labhsetwar, S. Devotta, Sol. Energy Mater. Sol. Cells 91 (2007) 180–190.

[32] C. Nasr, K. Vinodgopal, S. Kotchandani, A.K. Chattopadhyay, P.K. Kamat, Chem. Intermed. 23 (1997) 219–231.

[33] E. Pelizzetti, V. Carlin, C. Minero, M. Gratzel, M., New J. Chem. 15 (1991) 351–359.

[34] C. Minero, E. Pelizzetti, S. Malato, J. Blanco, Chemosphere 26 (1993) 2103–2119.

[35] G.V. Buxton, C.C. Greenstock, W.P. Helman, A.B. Ross, J. Phys. Chem. 17 (1988) 513–586.

[36] D. Nansheng, F. Tao, T. Shizhong, Chemosphere 33 (1996) 547–557.

[37] D. Behar, G. Czapki, I. Duchovny, J. Phys. Chem. 74 (1970) 2206–2210.

[38] M. Abdullah, G.K.C. Low, R.W. Matthews, J. Phys. Chem. 94 (1990) 6820–6825.

[39] D. Bockelmann, M. Linder, D. Bahnemann, Kulwer Academic Publishers, Netherlands, (1996) 675–689.

[40] S.T. Martin, A.T. Lee, M.R. Hoffmann, Environ. Sci. Technol. 29 (1995) 2567–2573.

[41] J. Kiwi, C. Pulgarin, P. Peringer, M. Graztel, New J. Chem. 17 (1993) 487–494.

[42] P. Pichat, C. Guillard, L. Amalric, A.C. Renard, O. Plaidy, Sol. Energy Mater. Sol. Cells 38 (1995) 391–399.

[43] N. Shimizu, C. Ogino, M.F. Dadjour, T. Murata, Sonochem. 14 (2007) 184–190.